Supporting Information

Defect ZrO$_{2-x}$ supported Ru nanoparticles as Mott-Schottky photocatalyst for efficient ammonia synthesis at ambient conditions

Rong Fu*[a, b, c], Yan Wang[a, b], Guangming Wang[d], Qingyun Zhan[c], Lili Zhang[c], Le Liu[c]

[a] School of Chemistry and Chemical Engineering, Liaocheng University, Liaocheng 252000, P. R. China

[b] Shandong Provincial Key Laboratory of Chemical Energy Storage and Novel Cell Technology, Liaocheng University, Liaocheng 252000, P. R. China

[c] State Key Laboratory of Inorganic Synthesis and Preparative Chemistry, College of Chemistry Jilin University, Changchun 130012, P. R. China

[d] Institute of Technology for Carbon Neutrality, Shenzhen Institute of Advanced Technology, Chinese Academy of Sciences Shenzhen, Shenzhen 518055, P. R. China

*Corresponding author's email: furong@lcu.edu.cn
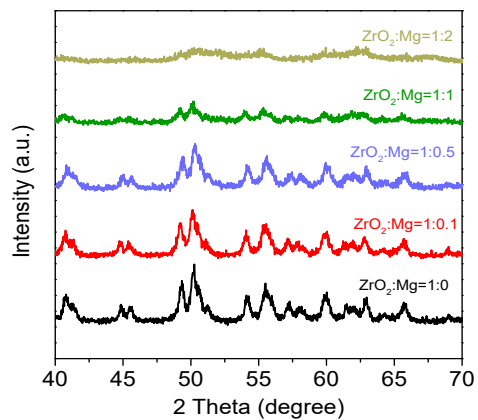
Fig. S1 Powder XRD patterns of ZrO_2 and various ZrO_{2-x} samples prepared with different molar ratio of ZrO_2 and Mg power.
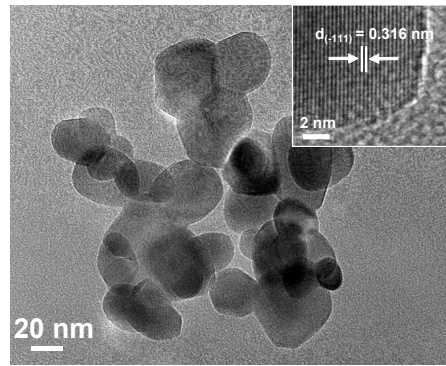
**Fig. S2** TEM image of ZrO$_2$. The inset shows the High-Resolution TEM image of ZrO$_2$.
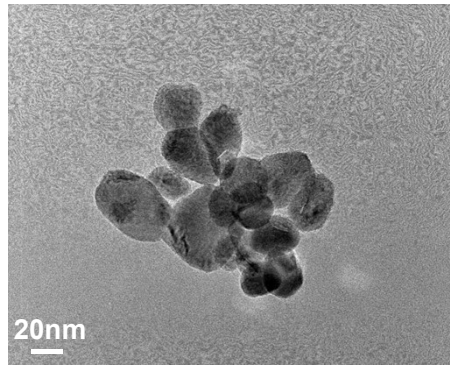
Fig. S3 TEM image of ZrO_{2-x}.
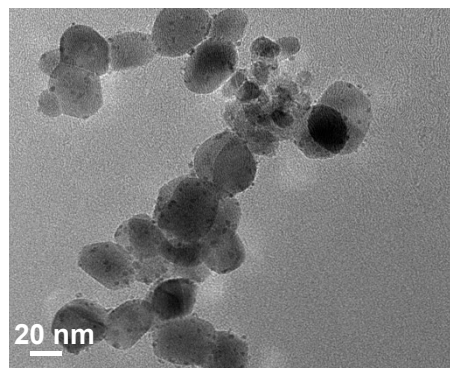
Fig. S4 TEM image of Ru@ZrO$_2$.
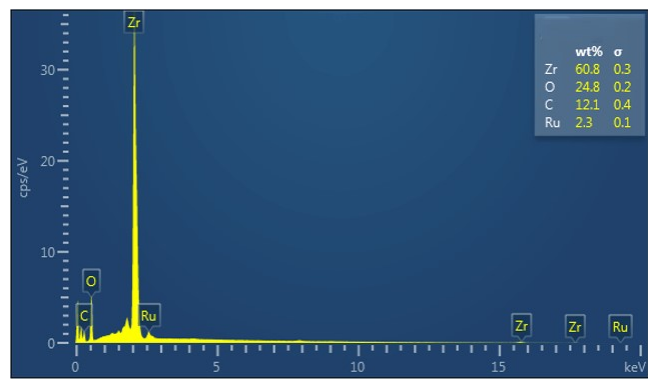
Fig. S5 EDS spectrum of Ru@ZrO$_{2-x}$.
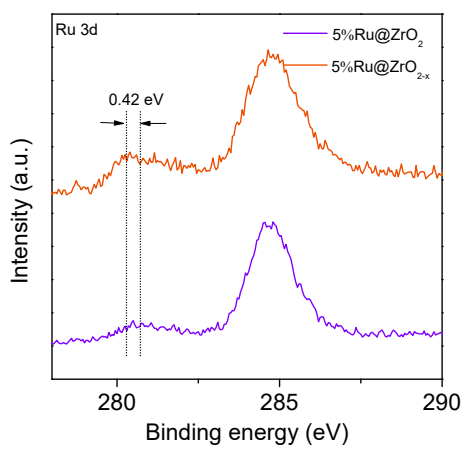
Fig. S6 XPS spectra of Ru 3d for Ru@ZrO$_2$ and Ru@ZrO$_{2-x}$.
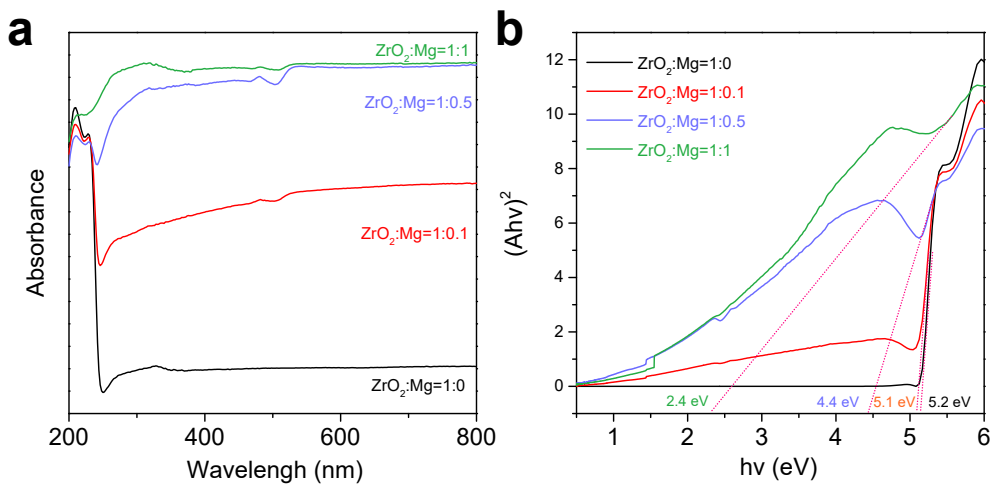
Fig. S7 (a) UV-VIS absorbance spectra of ZrO_2 and various ZrO_{2-x} samples prepared with different molar ratio of ZrO_2 and Mg power. (b) Band gap calculated from the fitting line using the Schuster-Kubelka-Munk equation with ZrO_2 and ZrO_{2-x} prepared with different molar ratio of ZrO_2 and Mg power.
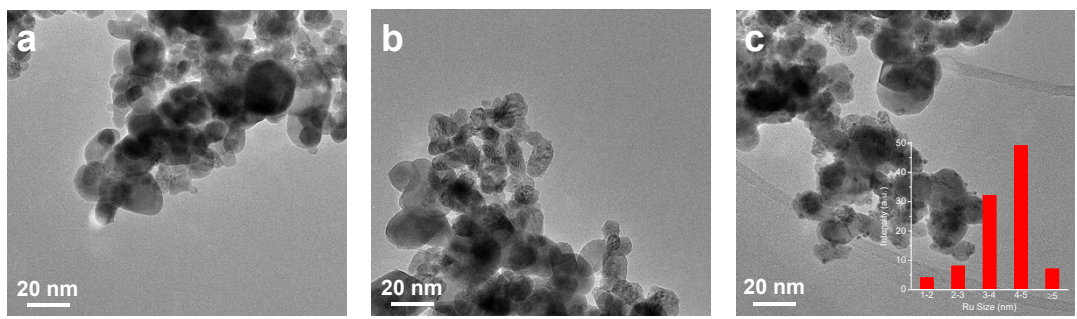
Fig. S8 TEM images of the as-synthesized (a) 1%Ru@ ZrO_{2-x}, (b) 2%Ru@ ZrO_{2-x}, (c) 10%Ru@ ZrO_{2-x}, the inset histogram shows the diameter distributions of Ru nanoparticles.
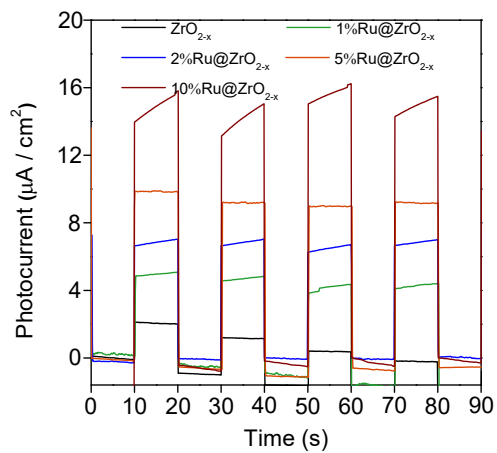
Fig. S9 The photocurrent responses of ZrO_{2-x}, $1\%Ru@ZrO_{2-x}$, $2\%Ru@ZrO_{2-x}$, $5\%Ru@ZrO_{2-x}$ and $10\%Ru@ZrO_{2-x}$.
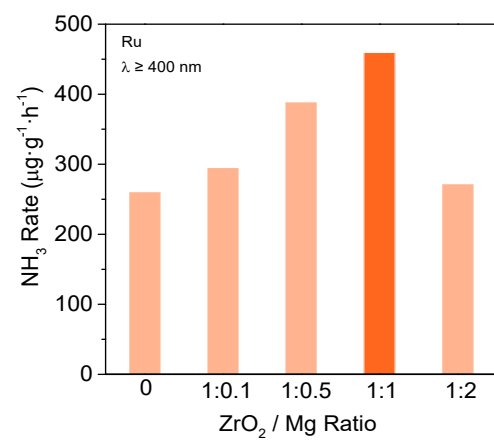
Fig. S10 Ammonia rate of catalysts prepared at different ZrO_2/Mg molar ratios with Ru nanoparticles.
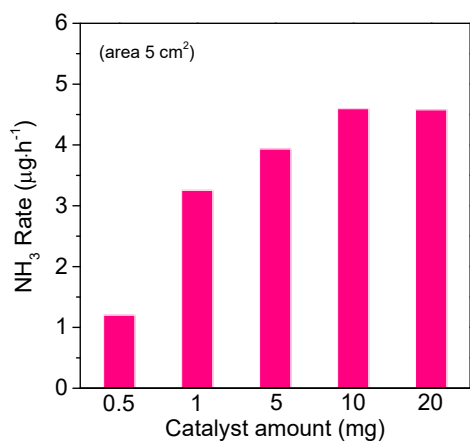
Fig. S11 Ammonia synthesis rate of Ru@ZrO$_{2-x}$ with different catalyst dosages.
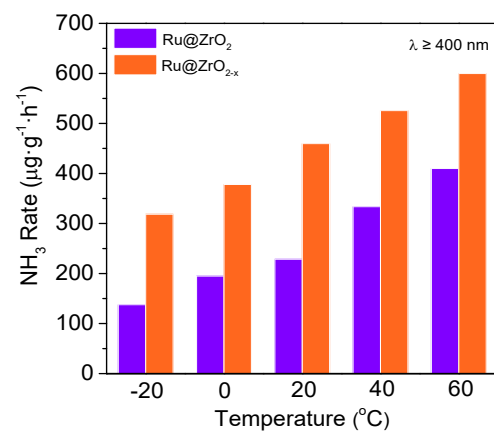
Fig. S12 The ammonia synthesis rate of Ru@ZrO$_2$ and Ru@ZrO$_{2-x}$ with different temperatures.
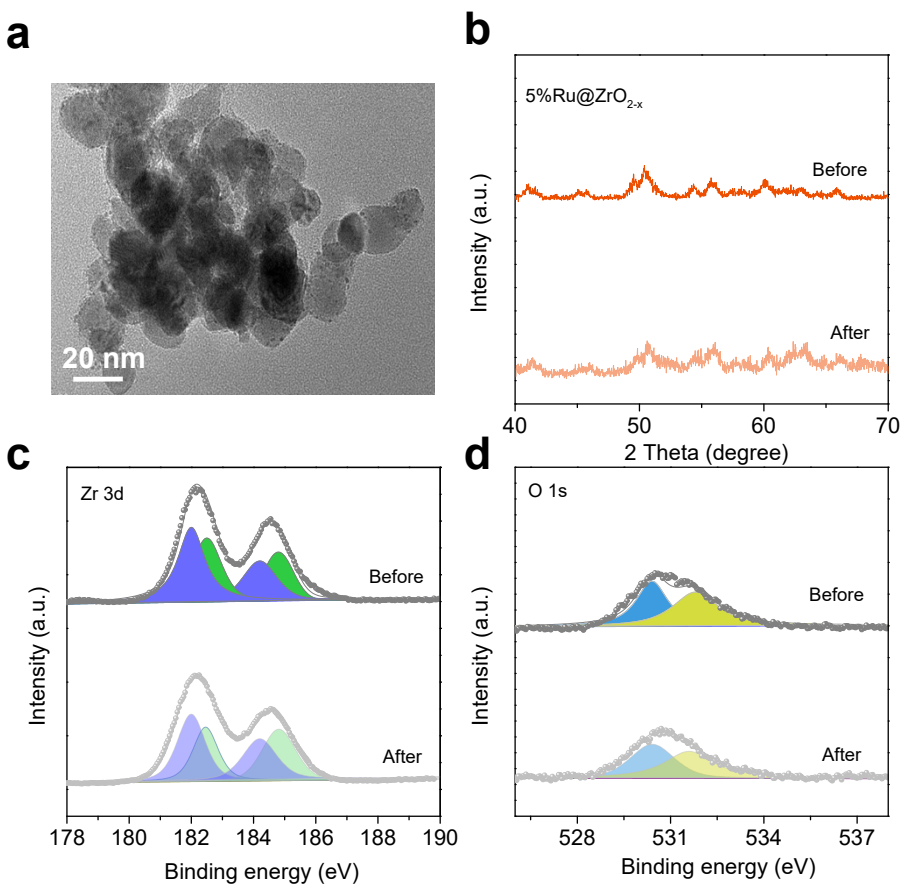
Fig. S13 Sample characterizations of 5%Ru@ZrO$_{2-x}$ after five cyclic tests for photocatalytic N$_2$ fixation: (a) TEM image; (b) XRD pattern; (c) XPS spectra of Zr 3d for 5%Ru@ZrO$_{2-x}$; (d) XPS spectra of O 1s for 5%Ru@ZrO$_{2-x}$.

In the associative mechanism of photocatalytic N_2 reduction, a continuous N_2 photoreductive protonation process is indispensable. The photogenerated holes will be neutralized by H_2 to form protons. Specifically:

$$(1) \quad 3H_2^* + 6h^+ \rightarrow 6H^+$$
$$(2) \quad N_2^* + e^- + H^+ \rightarrow N_2H^*$$
$$(3) \quad N_2H^* + e^- + H^+ \rightarrow NNH_2^*$$
$$(4) \quad NNH_2^* + e^- + H^+ \rightarrow N^* + NH_3$$
$$(5) \quad N^* + e^- + H^+ \rightarrow NH^*$$
$$(6) \quad NH^* + e^- + H^+ \rightarrow NH_2^*$$
$$(7) \quad NH_2^* + e^- + H^+ \rightarrow NH_3$$

Overall reaction: $3H_2^* + N_2^* + 6h^+ + 6e^- \rightarrow 2NH_3$
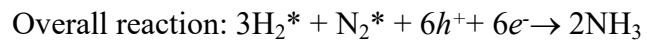
Fig. S14 Schematic diagram of the photocatalytic mechanism.
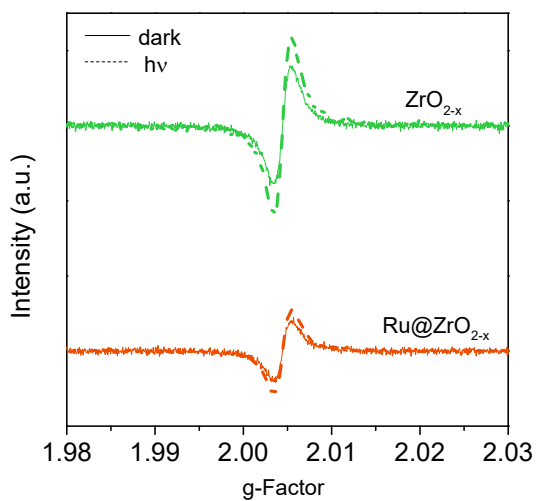
Fig. S15 In situ EPR spectra of ZrO_{2-x} and $Ru@ZrO_{2-x}$ under light irradiation in the presence of N_2 and H_2.

Table S1. The peaks parameters of O 1s for ZrO_2 and ZrO_{2-x}.

Sample	Name	BE (eV)	Area	O_V/O_L+O_V
ZrO_2	O-Lattice	530.3	58970	15.5%
	O-Vacancy	531.9	10800	
ZrO_{2-x}	O-Lattice	530.3	25993	55.4%
(ZrO_2 : Mg=1:1)	O-Vacancy	531.9	32264	

Table S2. The peaks parameters of E_g, E_{CB}, E_{VB}, E_f, and (vs Vacuum) for ZrO_2 and ZrO_{2-x}.

Sample	E_g (eV)	E_{CB} (eV)	E_{VB} (eV)	E_f (eV)
ZrO_2	5.2	-3.87	-9.07	-6.77
ZrO_{2-x}	2.4	-3.75	-6.25	-4.35

Determination of band edge positions of ZrO_2 and ZrO_{2-x}.

Relative E_{VB} positions were determined by the VB-XPS, and both ZrO_2 and ZrO_{2-x} exhibited an edge value of 2.3 eV and 2.1 eV. E_{CB} positions were calculated from Mott-Schottky plots, the flat-band potential values for ZrO_2 and ZrO_{2-x} were -0.71 V and -0.83 V (vs SCE), respectively. As SHE (V) can be transformed to physical scale (eV) according to $E_{phys} = - (E_{SHE} + 4.44)$, the flat-band potentials were located at -3.97 and -3.85 eV for ZrO_2 and ZrO_{2-x}, respectively. The values calculated were usually 0.1 eV higher than the flat band potential, the CB positions (E_{CB}) of ZrO_2 and ZrO_{2-x} were -3.87 and -3.75 eV (vs Vacuum). After calculating the bandgap (E_g) of ZrO_2 (5.2 eV) and ZrO_{2-x} (2.4 eV) from the UV-Vis-NIR spectra, E_{VB} positions were also determined through $E_{VB} = E_{CB} - E_g$ [1]. The peaks parameters of E_g, E_{CB}, E_{VB}, E_f, and (vs Vacuum) for ZrO2 and ZrO_{2-x}. were shown Table S2.

The apparent electron carrier concentrations

The apparent electron carrier concentrations of different catalysts can be calculated by Mott-Schottky curve and formula.

$$N_d= (2/e\varepsilon\varepsilon_0) \, [d(1/C^2)/dV]^{-1}$$

Where e is the electron charge, ε_0 is the vacuum permittivity, ε is the relative dielectric constant of the semiconductor material. C is the interfacial capacitance between the semiconductor and the electrolyte. $d(1/C^2)/dV$ represents the slope of the approximately linear part of the Mott Schottky curve.

Table S3. Representative works on photocatalytic nitrogen fixation.

Catalysts	Conditions	Temperature (K)	NH$_3$ rate (μg g^{-1} h^{-1})	Ref.
2%Ru@F-TiO$_{2-x}$	Visible light (400-800nm)	293	118.5	S2
2%Ru@WO$_{3-x}$	Visible light (400-800 nm)	293	27	S2
2%Ru@CeO$_{2-x}$	Visible light (400-800 nm)	293	32	S2
Defect TiO$_2$	$\lambda \geqslant 280$ nm	313	12.41	S3
3%FePt@g-C$_3$N$_4$	Visible light (400-800 nm)	293	63	S4
Fe-Al@graphene	UV light ($\lambda < 400$ nm)	473	430.1	S5
Ru@Ti-ZnO	Visible light (400-800 nm)	293	~240	S6
Ru@ZrO$_{2-x}$	Visible light (400-800 nm)	293	460	*This work*
Film-Ru@ZrO$_{2-x}$	Visible light (400-800 nm)	293	3256	*This work*

Supplementary References

[S1] C. Mao, L. Yu, J. Li, J. Zhao and L. Zhang., *Appl. Catal. B*, 2018, **224**, 612-620.
[S2] R. Fu, Z. W. Wu, Z. Y. Pan, Z. Y. Gao, Z. Li, X. H. Kong and L. Li, *Angew. Chem. Int. Ed.*, 2021, **60**, 11173-11179.
[S3] H. Hirakawa, M. Hashimoto, Y. Shiraishi and T. Hirai, *J. Am. Chem. Soc.*, 2017, **139**, 10929-10936.
[S4] Z. Li, Z. Y. Gao, B. W. Li, L. L. Zhang, R. Fu, Y. Li, X. Y. Mu and L. Li, *Appl. Catal. B*, 2020, **262**, 118276.
[S5] Y. Yang, T. Zhang, Z. Ge, Y. Lu and Y. Chen, *Carbon*, 2017, **124**, 72.
[S6] Z. Li, Z. Y. Pan, S. Cai, Z. Y. Gao, Z. L. Li, R. Fu, Z. H. Zhao, X. Y. Mu and L. Lu, *ACS Sustainable Chem. Eng.*, 2021, **9**, 13630-13639.